Molecular Crystals and Liquid Crystals Science and Technology. Section A. Molecular Crystals and Liquid Crystals

Publication details, including instructions for authors and subscription information:
http://www.tandfonline.com/loi/gmcl19

Magnetization of High-T_c Molecule-Based Magnet V/TCNE/CH_2Cl_2

W. B. Brinckerhoff [a], Jie Zhang [b], Joel S. Miller [b] & A. J. Epstein [c]

[a] Department of Physics, The Ohio State University, Columbus, OH, 43210-1106

[b] Department of Chemistry, University of Utah, Salt Lake City, UT, 84112

[c] Department of Physics and Department of Chemistry, The Ohio State University, Columbus, OH, 43210-1106

Version of record first published: 05 Dec 2006.

To cite this article: W. B. Brinckerhoff , Jie Zhang , Joel S. Miller & A. J. Epstein (1995): Magnetization of High-T_c Molecule-Based Magnet V/TCNE/CH_2Cl_2 , Molecular Crystals and Liquid Crystals Science and Technology. Section A. Molecular Crystals and Liquid Crystals, 272:1, 195-205

To link to this article: http://dx.doi.org/10.1080/10587259508055288

Mol. Cryst. Liq. Cryst., 1995, Vol. 272, pp. 195–205
Reprints available directly from the publisher
Photocopying permitted by license only

MAGNETIZATION OF HIGH-T_c MOLECULE-BASED MAGNET V/TCNE/CH_2Cl_2

W.B. BRINCKERHOFF
Department of Physics, The Ohio State University, Columbus, OH 43210-1106

JIE ZHANG and JOEL S. MILLER
Department of Chemistry, University of Utah, Salt Lake City, UT 84112

A.J. EPSTEIN
Department of Physics and Department of Chemistry, The Ohio State University, Columbus, OH 43210-1106

Abstract Room-temperature molecular magnets based on V/TCNE may be prepared via two routes, identified as $V(C_6H_6)_2$/TCNE/CH_2Cl_2 and $V(CO)_6$/TCNE/CH_2Cl_2. Both compounds have critical temperatures exceeding 350 K. The magnetization M(T,H) of samples prepared via both routes have been compared. The saturation magnetization of the $V(CO)_6$-derived material ($M_0 \sim 10^4$ emu•Oe•mol^{-1}) is larger than that observed for $V(C_6H_6)_2$-derived materials ($M_0 \sim 0.6 \times 10^4$ emu•Oe•mol^{-1}), and the behavior of M(T) at H = 100 Oe is more like that exhibited by crystalline magnets. Whereas $V(C_6H_6)_2$/TCNE/CH_2Cl_2 has a linear M(T) for $5 \leq T \leq 300$ K, the magnetization of $V(CO)_6$/TCNE/CH_2Cl_2 follows the Bloch spin-wave form $M(T) = M(0)(1 - BT^{3/2})$, where the zero-temperature magnetization M(0) is suppressed from M_0 by the effect of random magnetic anisotropy (RMA). The values of M(0) and the spin-wave dispersion constant B, as well as the range of validity of the $T^{3/2}$ law, vary among different preparations of the magnet, reflecting a correlation between magnetic and structural anisotropies. For the $V(CO)_6$-derived magnet, near $T_c \approx 370$ K, the large value of the critical exponent $\beta \approx 0.6$ reflects the presence of RMA, consistent with other V/TCNE systems. A scaling analysis is presented.

INTRODUCTION

The underlying origin of the dramatic two-order of magnitude increase in the critical temperature T_c of the first ambient-temperature molecule-based magnet $V(TCNE)_2$•½(CH_2Cl_2) (TCNE = tetracyanoethylene)[1] is intriguing for fundamental magnetism and also for the design of new materials. Future technological applications of molecule-based magnets, such as magnetic and electromagnetic shielding[2] and novel digital components, will require a detailed understanding of their unconventional physics and

precise control of necessary magneto-structural parameters.

The presence of disorder has an important effect on the bulk magnetic state as well as on the dynamic properties of molecule-based magnets, especially in the $V(TCNE)_x \cdot y(solvent)$ class of ferrimagnetic materials.[3-5] Depending on the spinless solvent used, the structural correlation length varies, being ~ 10 - 15 Å in the case of MeCN solvent and larger in the case of CH_2Cl_2 solvent.[6] By coordinating with V and/or acting as an interstitial spacer, the solvent directly affects the strength of the effective magnetic coupling between molecular units, leading to critical temperatures ranging from 80 to 400 K. Some of the results for three of the most thoroughly studied materials are summarized in Table I.

TABLE I Properties of $V(TCNE)_x \cdot y(solvent)$ for different solvents.

Solvent	T_c (K)	H_c^{RT} (Oe)	Proposed Role
CH_2Cl_2	350 - 400	15 - 60	spacer, possible ligand
C_4H_8O	190 - 205	≤ 20	spacer + ligand (V-O)
MeCN	80 - 150	0.2 - 0.5	spacer + ligand (V-CN)

In this report, we show that, in addition to the solvent used, the source of vanadium also has a profound effect on the resulting bulk magnetic state. We have studied the magnetization of the highest-T_c version prepared via two routes, identified as $V(C_6H_6)_2$/TCNE/CH_2Cl_2 and $V(CO)_6$/TCNE/CH_2Cl_2. While both routes yield a room-temperature bulk ferrimagnet, the material derived from $V(CO)_6$ has a higher saturation magnetization, depending on preparation, a slightly lower T_c, and a larger temperature range of validity of Bloch's Law than for the $V(C_6H_6)_2$-derived compound.

SAMPLE PREPARATION AND CHEMICAL ANALYSIS

The preparation of the V/TCNE magnets has been described in detail previously.[1,7] The addition of $V^0(C_6H_6)_2$ or $V^0(CO)_6$ to an excess of TCNE in dichloromethane at room temperature results in a black solid precipitate that is highly sensitive to air and moisture. Though the x-ray diffraction pattern for $V(CO)_6$/TCNE/CH_2Cl_2 is very similar to that of the material derived from $V(C_6H_6)_2$, the relative intensities of the diffraction peaks differ, indicating a variation in structural order.[6] Infrared absorption spectra of V/TCNE/CH_2Cl_2 prepared from $V(C_6H_6)_2$ and $V(CO)_6$ indicate similar elemental compositions but different binding modes. The carbonyl and benzene ligands are both absent from the products.

RESULTS

For the magnetization measurements we used both Faraday balance[8] and Quantum Design MPMS SQUID magnetometers. The powder samples, usually ~ 2 - 3 mg, were loaded into quartz tubes in an argon atmosphere and sealed under vacuum. The dominant source of uncertainty in both techniques was the sample mass, estimated to be correct within 0.1 mg.

Isothermal Magnetization

Figure 1 compares the isothermal magnetization M(H) of the magnets prepared from $V(CO)_6$ and $V(C_6H_6)_2$. The saturation magnetization M_0 ~ 10000 emu•Oe•mol^{-1} of the $V(CO)_6$ - derived compound (estimated from the measured moment in an applied magnetic field of 3 T) is larger than that of the material derived from $V(C_6H_6)_2$, M_0 ~ 6000 emu•Oe•mol^{-1}. For comparison, M_0 for a magnet with a repeat unit of net spin per formula unit of S = 1/2 and g = 2 is M_0 = 5585 emu•Oe•mol^{-1}. The magnetization of the $V(C_6H_6)_2$-derived material is thus in accord with V^{2+} (S = 3/2) antiferromagnetically coupled with two coordinating $(TCNE)^-$ anions (S = 1/2) per magnetic unit. However, such a coupling and stoichiometry does not account for the higher saturation of the $V(CO)_6$-derived material.

The approach to saturation varies among different preparations of $V(CO)_6$/TCNE/CH_2Cl_2, consistent with the variability of earlier-studied V/TCNE magnets. The extreme insolubility of the product and reactivity of synthetic components likely leads to a range of local structural order, reflected in the differing T_c values and magnetization characteristics. The data in Fig. 1 from two preparations of $V(CO)_6$/TCNE/CH_2Cl_2 exhibit the full range of variability observed.

The room-temperature hysteresis loops, Figure 2, show that the $V(CO)_6$-derived material saturates more quickly and has a smaller coercive field ($H_c \lesssim 15$ Oe) than the magnet derived from $V(C_6H_6)_2$ ($H_c \approx 60$ Oe).

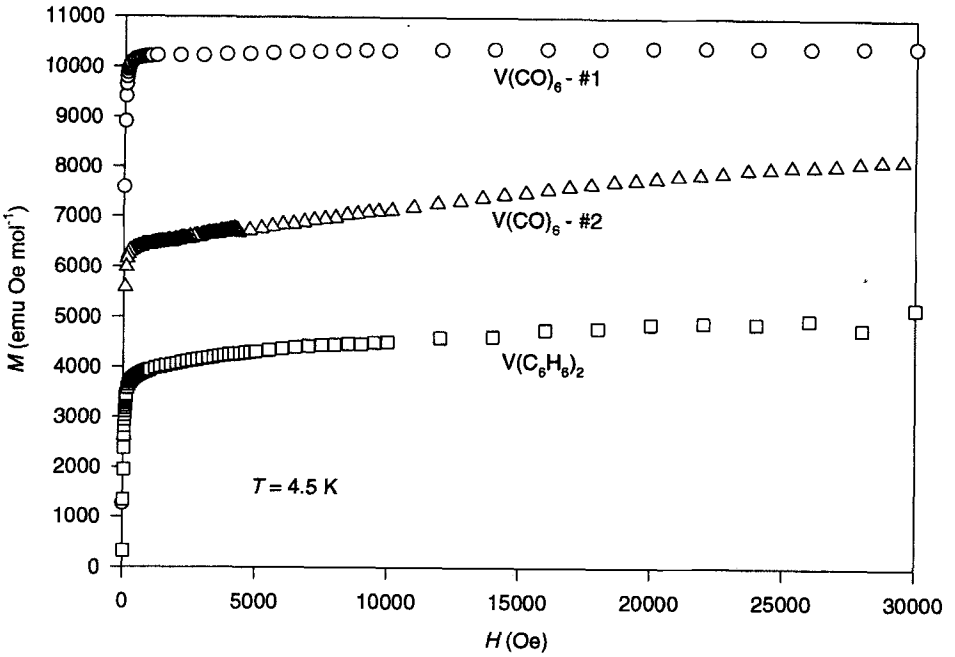

FIGURE 1 Isothermal magnetization of V/TCNE/CH_2Cl_2 from $V(CO)_6$ and $V(C_6H_6)_2$ sources. (SQUID magnetometer results).

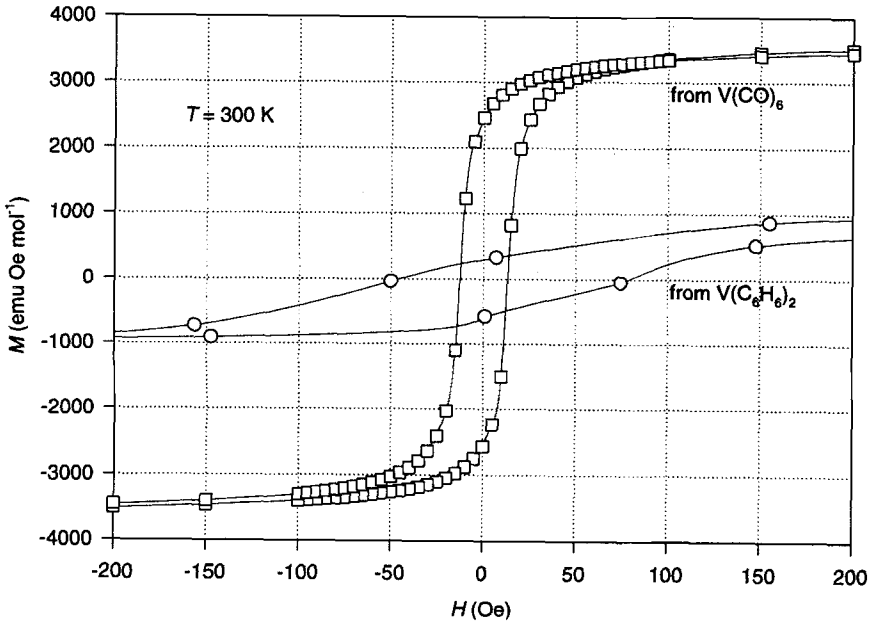

FIGURE 2 Room-temperature hysteresis of V/TCNE/CH_2Cl_2. (Materials from $V(CO)_6$ and $V(C_6H_6)_2$ measured with SQUID and Faraday techniques, respectively).

Temperature Dependence

The temperature dependence of the magnetization at low (100 Oe) and high (5000 and 2000 Oe) applied fields for the $V(CO)_6$ and $V(C_6H_6)_2$-derived materials, respectively, is shown in Figure 3. The curvature of M(T) for the $V(C_6H_6)_2$-derived system is highly suppressed consistent with disorder.[4,5] At low fields, the variation between preparations from $V(CO)_6$ is most pronounced. As the applied field is increased, the maximum magnetization obtained at low temperatures $M_S(T \rightarrow 0)$ increases.

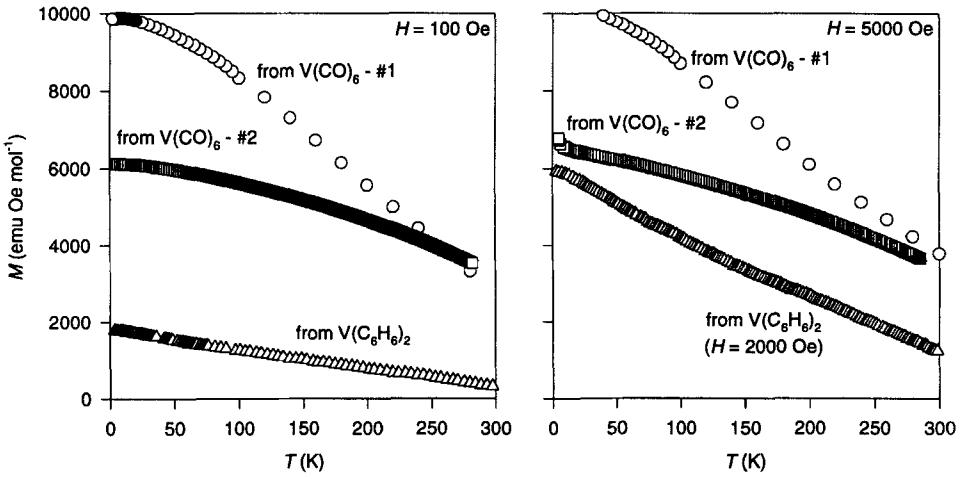

FIGURE 3 Temperature dependence of the magnetization at low (100 Oe) and high (5000 and 2000 Oe) applied fields for the $V(CO)_6$ and $V(C_6H_6)_2$-derived materials, respectively for V/TCNE/CH_2Cl_2 samples. The progression of overlapping data point symbols indicates the direction of temperature (warming or cooling) during measurement (e.g., the data presented for the $V(C_6H_6)_2$-derived material was taken during warming).

DISCUSSION

The qualitative picture that emerges from the M(T,H) data is that the magnetic behavior of the material derived from $V(CO)_6$ is that of a less-disordered magnet than the the data of the material from $V(C_6H_6)_2$, with variations occuring among different preparations. Insight into the "effective" increased order may be obtained via low-temperature spin-wave analysis and high-temperature analysis of the critical exponents.

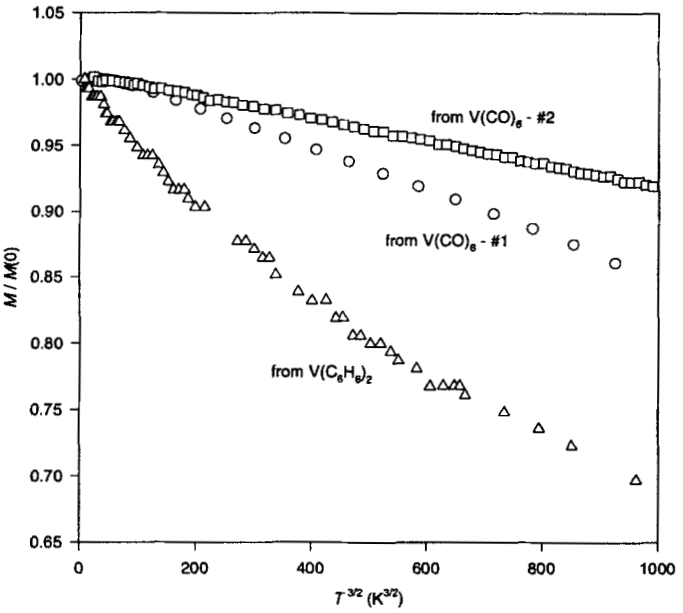

FIGURE 4 Reduced low-field magnetization versus $T^{3/2}$ for spin-wave analysis.

Low-Temperature Magnetization: Bloch's Law

Information about excited states, exchange coupling, and molecular coordination can be extracted from the low-temperature magnetization. At temperatures well below T_c the temperature dependence of the magnetization of a 3D ferro- or ferrimagnet generally is described by Bloch's Law, $M(T) = M(0)[1 - BT^{3/2}]$.[9] The constant B, deduced from the slope of M versus $T^{3/2}$ at low fields (Fig. 4), is related to the noninteracting magnon energy dispersion. For a simple-cubic ferromagnet with S = 1/2 at each site,

$$B^{FM} = \frac{1}{S}\left(\frac{k_B}{8\pi J^{FM} S}\right)^{\frac{3}{2}} \zeta\left(\frac{3}{2}\right) \approx 0.1173\left(\frac{k_B}{J^{FM}}\right)^{\frac{3}{2}}; \qquad S = \frac{1}{2},$$

while for a two-sublattice (e.g., $S_1 = 3/2$, $S_2 = 1/2$) model of a simple-cubic ferrimagnet,[10]

$$B^{FI} = \frac{2}{S_1 - S_2}\left(\frac{k_B(S_1 - S_2)}{16\pi J^{FI} S_1 S_2}\right)^{\frac{3}{2}} \zeta\left(\frac{3}{2}\right) \approx 0.0226\left(\frac{k_B}{J^{FI}}\right)^{\frac{3}{2}}; \qquad S_1 = \frac{3}{2},\ S_2 = \frac{1}{2}.$$

In these formulas, ζ is the Riemann zeta function and J^{FM} and J^{FI} are the ferro- and ferrimagnetic isotropic exchange couplings, respectively. Neither of these spin-wave models are expected to exactly reflect the low-temperature behavior of V/TCNE/CH_2Cl_2. However, as these compounds are strongly disordered, a three-sublattice model is unlikely to give substantial improvement.

The values of B obtained by fitting M(T) of V/TCNE/CH_2Cl_2 prepared from $V(C_6H_6)_2$ and $V(CO)_6$ to Bloch's Law for temperatures between 4 and 35 K, and 2 and 100 K, respectively, are shown in Table II, together with those for Fe and Ni. T_c^B is the critical temperature predicted by setting M = 0 in Bloch's Law ($T_c^B = B^{-2/3}$). The exchange coupling calculated from the spin-wave equations (1) and (2) are tabulated, together with the critical temperature estimated from the mean-field equation $3k_BT_c^{MFT} \approx 2Jz[S_1(S_1+1)S_2(S_2+1)]^{1/2}$ ($z \approx 6$ is the assumed average number of nearest neighbors). The observed values T_c^{exp} are also tabulated. It is noted that the predicted T_c^{MFT} is closer to the experimental value using the ferromagnetic model (Eq. 1) for the $V(C_6H_6)_2$-derived material and the ferrimagnetic model (Eq. 2) for sample #2 of the $V(CO)_6$-derived material. The observed T_c^{exp} for sample #1 of the $V(CO)_6$-derived material is mid-way between T_c^{MFT} predicted by the ferromagnetic and ferrimagnetic models.

TABLE II Bloch coefficient B, exchange coupling J, and critical temperatures T_c for V/TCNE and other magnets. See text for explanation of variables. Values for Fe and Ni are from Ref. 11.

Material	B ($K^{-3/2}$)	T_c^B (K)	J^{FM}/k_B (K)	$T_c^{MFT\text{-}FM}$ (K)	J^{FI}/k_B (K)	$T_c^{MFT\text{-}FI}$ (K)	T_c^{exp} (K)
V/TCNE/CH_2Cl_2							
... from $V(CO)_6$ #1	15×10^{-5}	354	85	570	28	189	~370
... from $V(CO)_6$ #2	8.5×10^{-5}	517	124	832	41	275	~370
... from $V(C_6H_6)_2$	40×10^{-5}	184	44	295	15	101	~400
Fe	0.34×10^{-5}	4423	205	2187	n/a	n/a	1043
Ni	0.75×10^{-5}	2610	230	920	n/a	n/a	631

The large values of B are a general feature of disordered magnets; typically B is a factor of two to four larger in amorphous ferromagnets than in related crystalline ferromagnets.[12] This trend is interpreted as a softening of the spin wave stiffness $D_a = 2JSa^2$, where a is the lattice constant. In disordered magnets, small-**q** spin waves are more easily excited and M decreases more quickly. The B-values of the V/TCNE magnets are consistent with such a description. The material prepared from $V(CO)_6$ does not simply behave as a "semi-crystalline" counterpart of the material from $V(C_6H_6)_2$. The temperature range of validity

of Bloch's Law is usually a factor of two or more larger in amorphous ferromagnets than in crystalline counterparts.[12] These ranges for $V(CO)_6$- and $V(C_6H_6)_2$-prepared V/TCNE magnets (~ 150 K and 60 K, respectively) are in opposition to this expectation. Despite these inconsistencies, the exchange constants J lead to critical temperatures within 25% of the observed values for some samples, suprisingly close for mean-field theory.

The deviation of M(T) of $V(C_6H_6)_2$/TCNE/CH_2Cl_2 from the usual Bloch's Law may reflect the role of random magnetic anisotropy (RMA). The RMA model has been applied[5] to the most disordered magnet in the V/TCNE class -- V/TCNE/MeCN. Within RMA there are randomly oriented easy-axes of magnetization, correlated over a length scale which depends sensitively on local chemical structure.[11-13] In a small magnetic field and when the strength of the RMA effect is much less than the intermolecular exchange J, there is a nonzero (average) magnetization which aligns with the magnetic field. At short length scales, the local magnetization vectors tilt slightly from the field direction toward the easy axes, i.e., it is a ferromagnet with a "wandering axis" (FWA). In such a regime, Bloch's Law fails due to the presence of a field-dependent gap $\Delta(H)$ in the magnon spectrum; spin waves are localized within the FWA correlation length. This localization results in highly suppressed magnetization curves, with $\Delta M \sim T$ in some cases, such as those observed in V/TCNE magnets.[5] The RMA model is also expected to apply to the present magnets made in CH_2Cl_2, with FWA correlation lengths larger than those made in MeCN. Further, spin-waves are likely more localized in the $V(C_6H_6)_2$-derived magnets than in the $V(CO)_6$-derived magnets, causing the increased deviation from Bloch's Law.

The presence of RMA in V/TCNE magnets may be viewed as an effect of local stoichiometric or chemical disorder induced by the random distribution of solvent molecules around the metal ion. Local stoichiometric variations may also give rise to a small variation in the exchange interactions between molecular units via a range of intermolecular distances. Such local effects may be present to varying degrees in the $V(C_6H_6)_2$- and $V(CO)_6$-derived magnets and lead to the strong differences in the M(T) curves. On the other hand, variations in the average stoichiometry can give rise to the range of saturation magnetizations M_S recorded in the M(H) data.

High-Temperature Magnetization: Critical Analysis

The critical scaling of the magnetization near the transition temperature provides information about the nature of the magnetic disorder in a system. The critical temperature $T_c \approx 400$ K of the $V(C_6H_6)_2$-derived materials prepared in CH_2Cl_2 is well above the thermal decomposition temperature $T_d \approx 350$ K, making the critical regime inaccessible. The $V(CO)_6$-derived compound prepared in CH_2Cl_2 has a lower critical temperature $T_c \approx 370$ K, with the same T_d. The determination of T_c and the availability of the critical regime

below T_c to measurement in this system depend upon the relative time scales of thermal decomposition and magnetization measurement. Above T_d, we assume M decays with an activated time constant,

$$M(t) = M(0)\, e^{-t/\tau(T)} \quad ; \quad \tau(T) \sim \exp(\Delta E/kT) ,$$

where t is time, τ^{-1} is the characteristic decomposition rate, and ΔE is an energy barrier related to the dissociation reaction kinetics that result in a loss of exchange coupling.

The magnetization was measured as a function of magnetic field at temperatures from 300 to 370 K. The time to increase the temperature between field runs was negligible compared to the M(H) scans. The corrections needed to account for the degradation of M, as determined by following the time dependence M(t) (at and above room temperature during field scans) were small, enabling estimation of the intrinsic magnetization in the range 350 - 370 K. The critical exponents β and δ, defined by

$$M \sim \left(\frac{T_c - T}{T_c} \right)^{\beta} \text{ as } T \to T_c \quad ; \quad M \sim H^{1/\delta} \text{ at } T_c ,$$

were evaluated utilizing log-log plots near T_c. The results, as well as the value of the susceptibility critical exponent γ calculated with Widom's scaling relation,[14] are summarized in Table III.

Table III Critical exponents for V/TCNE magnets. Values for the CH_2Cl_2 sample are those of the $V(CO)_6$ route. The data for MeCN and THF are from Refs. 4 and 13, respectively. Typical experimental values for crystalline[14] and amorphous[15] magnets are tabulated for comparison. Standard and RMA mean-field theory (MFT) values are given.

System	T_c (K)	β	δ	$\gamma = \beta(\delta-1)$
V/TCNE/CH_2Cl_2	~ 370	0.6	5	2.52
V/TCNE/THF	190 - 205	0.95	3.5	2.38
V/TCNE/MeCN	120 - 150	0.75	4	2.25
MFT		0.5	3	1
RMA MFT		0.75	1.67	0.5
Crystalline (typ.)		0.32-0.39	4-5	1.3-1.4
Amorphous (typ.)		0.38-0.44	4-5	1.3-1.7

The very large values of β in the V/TCNE magnets reflect the strong supression of the magnetization near T_c as compared to the behavior of more typical magnets. The small

increase in β expected when going from crystalline to amorphous systems may play a role in V/TCNE magnets but is not sufficient to explain the observed data. However, the effect of a weak random magnetic anisotropy is to increase β by 50% over the non-RMA case.[16] The value of $\beta \approx 0.6$ observed in $V(CO)_6/TCNE/CH_2Cl_2$ is consistent with the critical RMA effect on a typical disordered system with $\beta = 0.4$. The values of γ, which describe the divergence of the linear (in magnetic field) magnetic susceptibility near T_c according to $\chi \sim (1 - T/T_c)^{-\gamma}$, increase monotonically with correlation length. This trend is remarkable in that it describes sharper transitions (larger γ) in V/TCNE magnets with increased local structural order. As the values for δ are near those observed in crystalline magnets, the large values of γ likely reflect the enhancement of β from RMA. The measured magnitudes of β and γ may also be increased in disordered magnets by scaling outside the experimentally inaccessible core critical region.[15,17]

CONCLUSION

The magnetization M(T,H) of the room-temperature molecule-based magnet $V/TCNE/CH_2Cl_2$ has been compared for materials prepared from $V(C_6H_6)_2$ and $V(CO)_6$. Significant differences in magnetic behavior are found which indicate that the $V(CO)_6$-derived magnet is more ordered locally than the $V(C_6H_6)_2$-derived magnet, although the metal ligands are not in either final compound. A low temperature spin-wave analysis supports the view of increased order, although the magnet derived from $V(CO)_6$ is not simply a more crystalline version of the $V(C_6H_6)_2$-derived magnet.

The range of isothermal magnetization M(H) data and the critical scaling analysis near T_c suggest the presence of weak random magnetic anisotropy in $V(CO)_6/TCNE/CH_2Cl_2$. Critical exponents are consistent with the trend of V/TCNE magnets with increasing structural order having decreasing RMA strengths. Further magnetization and a.c. susceptibility studies are in progress to further probe the critical regimes of the V/TCNE/solvent class.

ACKOWLEDGEMENT

The authors gratefully acknowledge the support of the U.S. Department of Energy, DOE DMS DE-FG-86BR45271 and DOE DMS DE-FG03-93ER45504.

REFERENCES

1. J.M. Manriquez, G.T. Yee, R.S. McLean, A.J. Epstein, and J.S. Miller, Science 252, 1415 (1991).
2. B.G. Morin, C. Halm, J.S. Miller, and A.J. Epstein, J. Appl. Phys. 75, 5782 (1994).
3. K.S. Narayan, B.G. Morin, J.S. Miller, and A.J. Epstein, Phys. Rev. B 46, 6195 (1992).
4. P. Zhou, B.G. Morin, J.S. Miller, and A.J. Epstein, Phys. Rev. B 48, 1325 (1993).
5. P. Zhou, J.S. Miller, and A.J. Epstein, Phys. Lett A 189, 193 (1994).
6. J.P. Pouget, J.S. Miller, and A.J. Epstein, unpublished.
7. J. Zhang, P. Zhou, W.B. Brinckerhoff, A.J. Epstein, C. Vasquez, R.S. McLean, and J.S. Miller, submitted.
8. S. Chittipeddi, K.R. Cromack, J.S. Miller, and A.J. Epstein, Phys. Rev. Lett. 58, 2695 (1987).
9. F. Bloch, Z. Physik 61, 206 (1931); C. Kittel, Introduction to Solid State Physics, 6th Ed. (J. Wiley, N.Y., 1986), p.435.
10. J. Van Kranendonk and J.H. Van Vleck, Rev. Mod. Phys. 30, 1 (1958).
11. C.-W. Chen, Magnetism and Metallurgy of Soft Magnetic Materials, Dover, Mineola, New York (1986).
12. T. Kaneyoshi, Introduction to Amorphous Magnets, World Scientific, Singapore (1992).
13. P. Zhou, S.M. Long, J.S. Miller, and A.J. Epstein, Phys. Lett. A 181, 71 (1993).
14. K. Huang, Statistical Mechanics, Wiley, New York (1987), p.398.
15. T. Kaneyoshi, Amorphous Magnetism, CRC Press, Boca Raton (1984), sec. 5.4.
16. P.M. Gehring, M.B. Salamon, A. del Moral, and J.I. Arnaudas, Phys. Rev. B 41, 9134 (1990).
17. S.J. Poon and J. Durand, Phys. Rev. B 16, 316 (1977).